Fermi National Accelerator Laboratory

FERMILAB-Conf-95/046-E
E665

Proton and Deuteron Structure Functions in Muon Scattering at 470 GeV

Ashutosh V. Kotwal
For the E665 Collaboration

Fermi National Accelerator Laboratory
P.O. Box 500, Batavia, Illinois 60510

Department of Physics, Harvard University
Cambridge, MA 02138

May 1995

Proceedings of the *XXXth Rencontres de Moriond, QCD and High Energy Interactions*, Les Arcs, France, March 19-26, 1995.

Operated by Universities Research Association Inc. under Contract No. DE-AC02-76CHO3000 with the United States Department of Energy

Disclaimer

This report was prepared as an account of work sponsored by an agency of the United States Government. Neither the United States Government nor any agency thereof, nor any of their employees, makes any warranty, expressed or implied, or assumes any legal liability or responsibility for the accuracy, completeness, or usefulness of any information, apparatus, product, or process disclosed, or represents that its use would not infringe privately owned rights. Reference herein to any specific commercial product, process, or service by trade name, trademark, manufacturer, or otherwise, does not necessarily constitute or imply its endorsement, recommendation, or favoring by the United States Government or any agency thereof. The views and opinions of authors expressed herein do not necessarily state or reflect those of the United States Government or any agency thereof.

PROTON AND DEUTERON STRUCTURE FUNCTIONS IN MUON SCATTERING AT 470 GeV

Ashutosh V. Kotwal
Department of Physics, Harvard University,
Cambridge, MA 02138, U.S.A.
Representing the Fermilab E665 Collaboration.

ABSTRACT

The proton and deuteron structure functions F_2^p and F_2^d are measured in inelastic muon scattering with an average beam energy of 470 GeV. The data were taken at Fermilab experiment 665 during 1991-92 using liquid hydrogen and deuterium targets. The F_2 measurements are reported in the range $0.0008 < x < 0.6$ and $0.2 < Q^2 < 75$ GeV^2. These are the first precise measurements of F_2 in the low x and Q^2 range of the data. The E665 data overlap in x with the HERA data, and there is a smooth connection in Q^2 between the two data sets. At high Q^2 the E665 measurements are consistent with QCD-evolved leading twist structure function models. The data are qualitatively described by structure function models incorporating the hadronic nature of the photon at low Q^2. The Q^2 and the W dependence of the data measure the transition in the nature of the photon between a point-like probe at high Q^2 and a hadronic object at low Q^2.

1. Introduction

In the single photon exchange approximation the double differential cross-section for lepton-nucleon scattering can be written as

$$\frac{d^2\sigma_{1\gamma}}{d(-Q^{-2})d(lnx)} = 4\pi\alpha_{em}^2 F_2(x,Q^2)[1-y-\frac{Mxy}{2E}+\frac{y^2(1+4M^2x^2/Q^2)}{2(1+R(x,Q^2))}] \quad (1)$$

where E is the incoming lepton energy in the lab frame, and $-Q^2$ is the square of the 4-momentum transferred from the lepton. In the lab frame ν is the lepton energy loss, $x = Q^2/2M\nu = x_{Bj}$ is the Bjorken scaling variable, and $y = \nu/E$. α_{em} is the electromagnetic coupling constant and M is the nucleon mass. $F_2(x,Q^2)$ is the structure function of the target nucleon and $R(x,Q^2)$ is the ratio of the longitudinal to the transverse virtual photon cross-sections.

The experimental apparatus has been described elsewhere[1,10] . The data used for the structure function measurement are from the 1991-92 run. A muon beam of mean energy 470 GeV impinged on cryogenic liquid hydrogen and deuterium targets, and on an evacuated vessel. The empty target data are used to subtract the contribution of the out-of-target scatters on a statistical basis.

The trigger system includes two kinds of muon triggers, the small angle trigger (SAT), and the set of large angle triggers (LAT). In addition a trigger (CAL) based on the calorimeter signals was available. The small angle trigger used a floating veto so that it could also trigger on events where the scattered muon remained within the phase space of the beam. The trigger acceptance extended to scattering angles as small as 1 mrad.

2. Motivation

The behavior of the structure function F_2 is expected to be different in the small and large Q^2 limits. In the limit $Q^2 \to \infty$ we expect approximate scaling due to point-like photon-parton interactions, with an increase at low x_{Bj} and logarithmic scale dependence introduced by QCD radiative effects. In the QCD-improved parton model, photon-nucleon scattering at lower Q^2 may have a significant contribution from "higher-twist" effects in addition to the QCD radiative effects. Higher twist terms may formally be defined as terms inversely proportional to increasing powers of Q^2 in an expression for the photon-nucleon cross-section. These terms can be interpreted as the photon scattering off multi-parton states, or as the struck parton re-interacting with other partons in the nucleon.

Apart from the QCD-improved parton model, the photon-nucleon scattering process has also been described in the nucleon rest frame, in which it occurs mainly due to the interaction of the hadronic component of the photon with the nucleon. Furthermore, the Vector Meson Dominance (VMD) model states that the spectrum of the hadronic component is dominated by the low mass vector mesons, resulting in a strong Q^2 dependence (through vector meson propagators and the gauge invariance constraint) and only a weak x_{Bj} dependence at fixed Q^2. In the photoproduction limit, $\lim_{Q^2\to 0} F_2 = \sigma_{\gamma N}Q^2/4\pi^2\alpha$, where the factor of Q^2 is obtained from gauge invariance and $\sigma_{\gamma N}$ is the real photon-nucleon cross-section.

The Generalized Vector Meson Dominance (GVMD) model includes the contribution of higher mass states. In GVMD, the high mass hadronic components of the photon would correspond to highly virtual $q\bar{q}$ states, corresponding to spatially small color dipoles. The dipole field would reduce as the dipole shrinks with increasing Q^2, resulting in a diminishing cross-section with the nucleon. This is the idea of the "shrinking-photon" or "color-transparency", which restores the scaling behaviour of the structure function at high Q^2 in GVMD (for a review see[2]).

The measurement of the structure function extending from low to high Q^2 can help to illuminate the transition in the photon-nucleon scattering mechanism between the high and low Q^2 limits.

3. Experimental Issues

In order to extract the structure function from the event rates, the absolute luminosity, radiative corrections and apparatus effects must be known. The apparatus acceptance, trigger and reconstruction efficiencies, and smearing corrections are calculated using a Monte Carlo simulation of the detector. The simulation is tuned extensively and validated by performing many cross-checks against the data. The absolute luminosity is calculated by measuring the length, temperature and pressure of the liquid targets, counting the total number of beam muons, and using the random beam trigger method for normalization.

The experimentally measured quantity is the total muon double differential cross-section. In order to extract F_2, electromagnetic radiative corrections must be applied, and R must be known. For the analysis presented here, radiative corrections are calculated by the computer program FERRAD35[3] according to the formulation of Mo and Tsai.[4] The input F_2 is constructed from published fits[5–7] to SLAC, DESY, Daresbury and NMC data and the low Q^2 interpolation at high W^2 of Donnachie and Landshoff.[8] R is taken as R_{slac}.[9] The H_2 and D_2 event rates are corrected and normalized using an event-by-event weighting procedure. A fit to the resulting F_2 measurement is used to constrain the input F_2 in the low x range of the E665 data ($x < 0.05$). The detector acceptance and the radiative correction is recalculated in an iterative procedure until convergence is achieved.

Events used for the structure function measurement are required to have the beam energy between 350 and 600 GeV, $\nu > 35$ GeV, $\delta\nu/\nu < 0.5$ and the energy of the scattered muon greater than 100 GeV. As we have not yet fully understood the detector efficiency at large scattering angles, we have also required that $\theta_{scat} < 20$ mrad in this analysis. This removes some data at high x and Q^2, where the statistical precision was low to begin with. SAT events are used for the analysis. The kinematics of the event are determined from the 4-momenta of the beam and the scattered muon at the reconstructed vertex. The details of the structure function analysis may be found in[10] .

4. Results

The F_2 results for the proton are shown in figure 1. The errors shown are the statistical and kinematics-dependent systematic uncertainties added in quadrature, but the overall normalization uncertainty of 1.8% is not included. The statistical errors are 3-5% at low x and Q^2, and 20-30% at the highest x and Q^2 of the data. The total kinematics-dependent systematic uncertainty varies between ~2-10%. This includes uncertainties in the trigger efficiency ~1-5%, reconstruction efficiency ~1-8%, effect of energy scale uncertainty ~0-4%, radiative correction ~0-3%, effect of variation in R_{slac} <3%, and binning errors which are typically less than 1% (except edge bins). The maximum radiative correction is ~45% and agrees with the calculation[11] using the method of Bardin *et al* to ~2%. The difference between the Mo-Tsai calculation and the Bardin *et al* calculation is included in the systematic uncertainty, as is the change in the radiative correction due to variation in the input F_2 due to measurement error. The difference between F_2 obtained using R_{slac} and other functions for R ($R = 0$, R_{QCD}, using the modified low Q^2 MRS(A) parton distributions[12]) is typically small except at low x and high y where it is up to 10%. The results for the deuteron F_2 are similar, but with smaller statistical errors. The overall normalization uncertainty in F_2^d is 1.9%.

The measurement covers the range $8 \times 10^{-4} < x_{Bj} < 0.6$ and $Q^2 > 0.2$ GeV^2. In figure 1 on the left, the data in the low x range are compared with three structure function models.

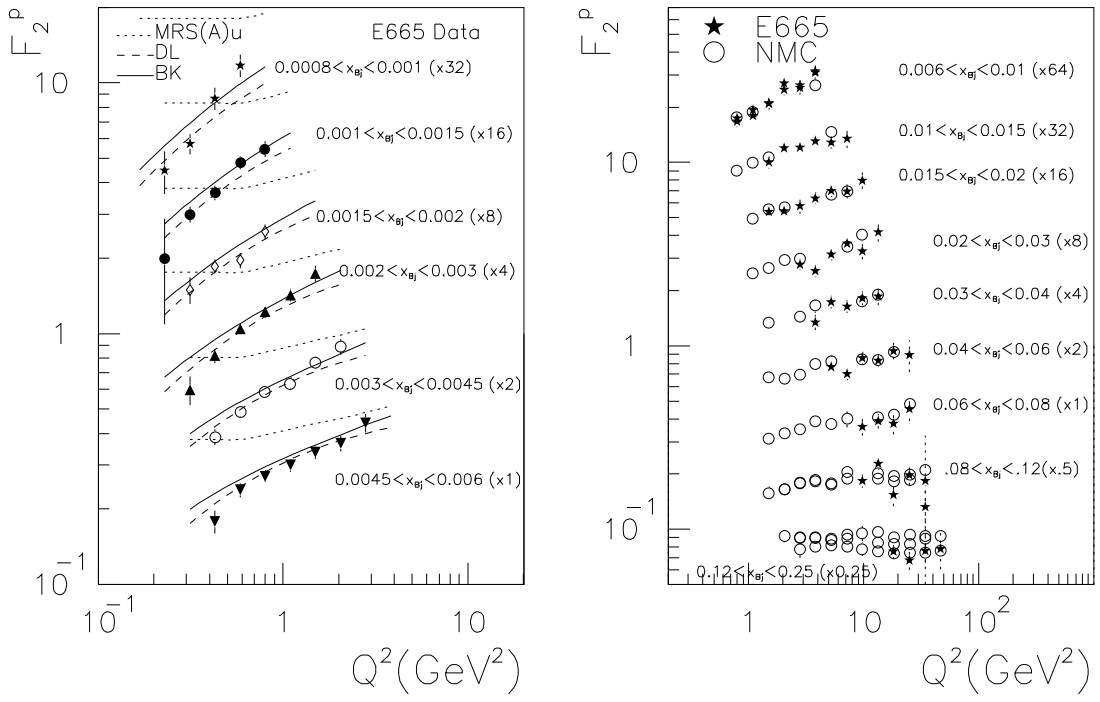

Fig. 1. F_2^p as a function of Q^2 in x_{Bj} bins. The errors shown are the statistical and systematic uncertainties added in quadrature, but the normalization uncertainty is not included. On the left, the E665 data at low x are compared with model calculations of Donnachie-Landshoff (DL), Badełek-Kwieciński (BK) and the MRS(A) parton distributions. On the right the E665 data at higher x are compared with the NMC data.

The MRS(A) curves are computed[12] by performing QCD evolution of leading-twist parton distributions both up and down in Q^2 from $Q_0^2 = 4GeV^2$. The Donnachie-Landshoff (DL) model[8] performs a phenomenological interpolation between the real photoproduction data and the NMC data below Q^2 of 10 GeV^2. It is designed to reproduce F_2 in the photoproduction limit, and approach a scaling function at high Q^2. The Badełek-Kwieciński (BK) model[13] merges the contribution from the ρ, ω and ϕ to F_2 with the partonic contribution using GVMD ideas. The MRS(A) curves are unable to reproduce the magnitude and slope of the data at low Q^2. Assuming that the difference is due to the higher-twist contribution, the comparison indicates that the higher-twist contribution is negative at low Q^2, and that it grows in magnitude with decreasing x and Q^2. The DL and BK models, which incorporate the hadronic nature of the photon at low Q^2, give a fairly good description of the data.

In figure 1 on the right, the E665 data in the higher x range are compared with the NMC data.[7] When a certain x bin is split by either experiment, the multiple data points are shown in that bin. Assuming only an overall normalization difference, the two measurements are consistent within normalization uncertainties.

The x_{Bj} values at E665 are comparable to those obtained at HERA and extend to lower values than those achieved at previous fixed target experiments. In figure 2 on the left, a subset of the E665 proton data is plotted in the corresponding x bins with the ZEUS data.[14] The BK model calculation is used to guide the eye in connecting the data from the two experiments as a function of Q^2 in each x bin. The plot shows that the data from the two experiments connect smoothly in Q^2. The x dependence at fixed Q^2 (and hence the W dependence, where W is the photon-nucleon c.m.s. energy) is weaker at low Q^2 that it is at high Q^2.

In figure 2 on the right, the virtual photon-proton cross-section (computed from F_2 using

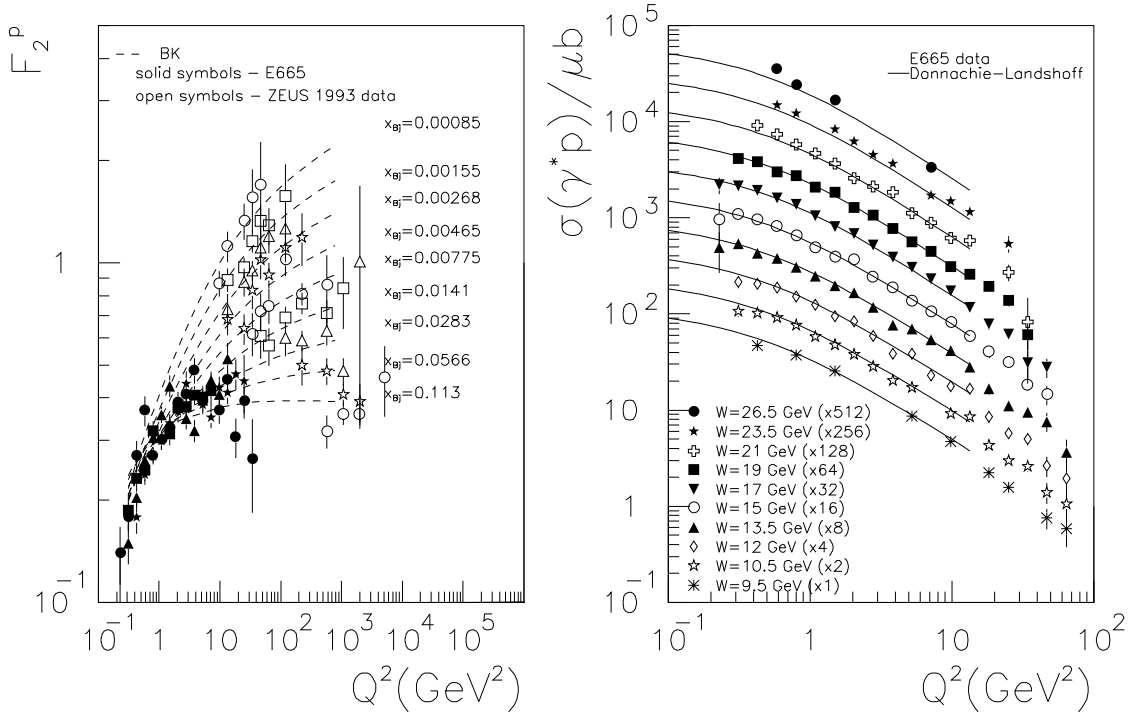

Fig. 2. (left) F_2^p vs Q^2 for different x_{Bj}, from E665 and ZEUS, with BK model calculation. (right) Virtual photon-proton cross-section vs Q^2 for different W, with DL model calculation.

the Hand convention for the photon flux $K = \frac{W^2-M^2}{2M}$) is shown versus Q^2 in bins of W. The Q^2 dependence becomes weaker as one goes from high to low Q^2. This is another way of visualizing the transition from the partonic to the hadronic scattering mechanism. The DL model which incorporates this transition is able to reproduce the trends in the data.

In figure 3 we show the logarithmic partial derivatives of the proton F_2 with respect to Q^2 and x respectively, holding the other variable fixed. On the left, $\partial ln F_2^p / \partial ln Q^2$ at fixed x is shown versus x, for the E665 data and the DL model. The data follow the trend in the model in the approach to the photoproduction limit (value of 1.08 obtained from[8]), however the slopes in the data tend to exceed the model prediction. On the right, $\partial ln F_2^p / \partial ln x$ at fixed Q^2 is shown versus Q^2, along with the photoproduction limiting value of -0.08 (obtained from[8]). The typical value of the slope (~ -0.3) observed in the higher Q^2 HERA data is also indicated (see[12] for a discussion). The x dependence at fixed Q^2 (hence the W dependence) of the E665 data is bounded by the higher and lower Q^2 measurements, thereby measuring the transition between the two.

5. Summary and Conclusions

We have presented measurements of the proton and deuteron structure functions F_2 in the kinematic range $x > 0.0008$ and $Q^2 > 0.2$ GeV^2. These are the first precise measurements of F_2 at such low x and Q^2. The data were obtained using a muon beam of average momentum 470 GeV, and liquid hydrogen and deuterium targets at the experiment 665 during 1991-92 at Fermilab.

The E665 measurements have a significant overlap in x and Q^2 with the measurements from NMC. In the region of overlap the two measurements are in good agreement. The E665 measurements also overlap in x with the HERA data, the E665 data being at lower Q^2 at fixed x. There is a smooth connection in Q^2 over a large range between the two data sets.

The E665 data show a transition in the nature of the photon-nucleon interaction when $Q^2 \sim \mathcal{O}(0.5\ \text{GeV}^2)$. While perturbative QCD evolution-based models give a good description of

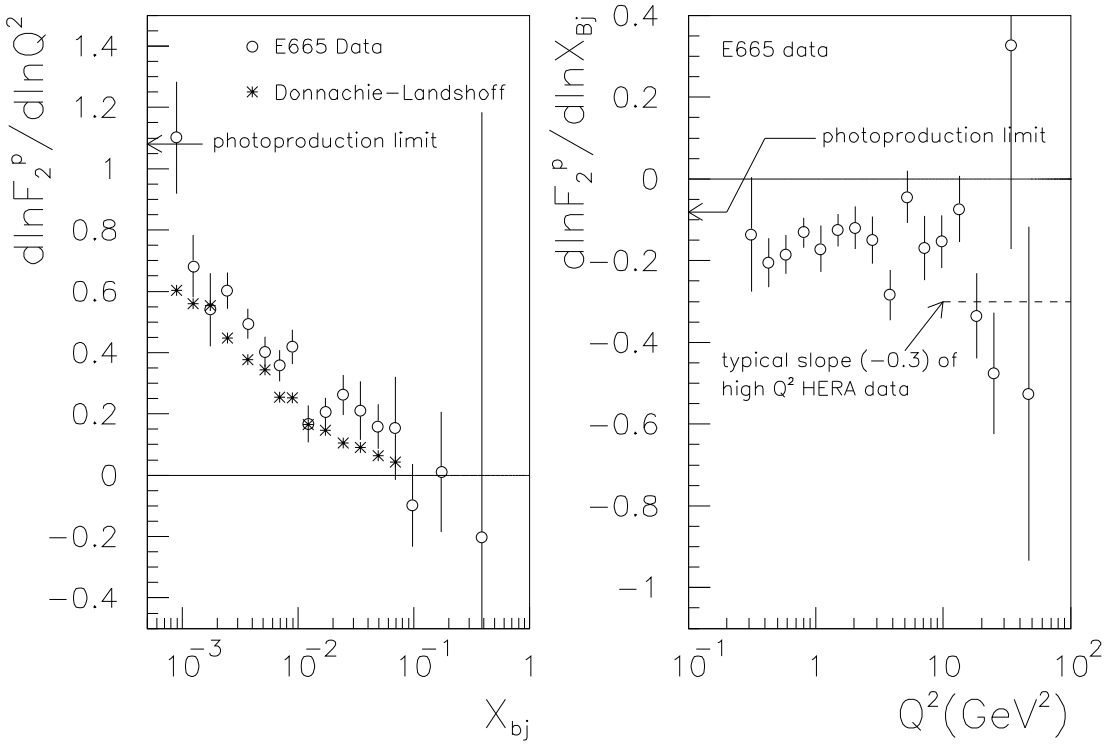

Fig. 3. (left) $\partial lnF_2^p/\partial lnQ^2$ at fixed x versus x, for the E665 data and the DL model. The value in the photoproduction limit, derived from the DL model, is also indicated. (right) $\partial lnF_2^p/\partial lnx$ at fixed Q^2 vs Q^2 for the E665 data.

the data at higher Q^2, they fail to describe the data at lower Q^2. Thus the data can be used to quantify the higher-twist effects as a function of x and Q^2. Models that incorporate the hadronic nature of the photon at low Q^2 are able to describe qualitatively the W and Q^2 dependence of the data. We find that at low Q^2, the W dependence of our data is stronger than that of real photoproduction and hadroproduction cross-sections, but weaker than the W dependence of the high Q^2 HERA data. Thus the data provides a measurement of the transition between high and low Q^2 in both the W and the Q^2 dependence of the photon-nucleon interaction mechanism.

References

1. M.R. Adams, *et al., Nucl. Inst. Methods* **A291** (1990) 533.
2. T. H. Bauer, R. D. Spital, D. R. Yennie and F. M. Pipkin, Reviews of Modern Physics, Vol. 50, No. 2, April 1978.
3. P. Amaudruz *et al., Nucl. Phys.* **B273** (1992) 3.
4. L.W. Mo and Y.S. Tsai, *Rev. Mod. Phys.* **41** (1969) 205.
5. F. W. Brasse *et al., Nucl. Phys.* **B39** (1972) 421-431.
6. F. W. Brasse *et al., Nucl. Phys.* **B110** (1976) 413.
7. New Muon Collaboration, *Phys. Lett.* **B295** (1992) 159-168.
8. A. Donnachie and P.V. Landshoff, *Z. Phys.* **C61** (1994) 139.
9. L.W. Whitlow *et al., Phys. Lett.* **B250** (1990) 193.
10. Ashutosh V. Kotwal, Ph.D. Thesis, Harvard University, Cambridge, USA, May 1995.
11. B. Badełek *et al.*, Preprint TSL/ISV-94-0092.
12. A.D. Martin, R.G. Roberts and W.J. Stirling, University of Durham preprint DTP/94/78 (1994). Fortran code to calculate F_2 and R kindly provided by Dr. W. J. Stirling.
13. B. Badełek and J. Kwieciński, Phys. Lett. B295, 263 (1992). Fortran code to calculate the structure functions kindly provided by Dr. B. Badelek.
14. ZEUS Collaboration, DESY preprint 94-143, August 1994.